

A Monte-Carlo and Self-Consistent Field calculations of encapsulated spherical polymer brushes.

Juan J. Cerdà, Tomás Sintés and Raúl Toral *

Departament de Física and IMEDEA (CSIC-UIB).

Universitat de les Illes Balears. 07122 Palma de Mallorca, Spain.

(Dated: November 13, 2018)

We present the results of extensive numerical self-consistent field (SCF) and 3-dimensional off-lattice Monte Carlo (MC) studies of a spherical brush confined into a spherical cavity. The monomer density profile and the cavity pressure have been measured in systems where curvature of the cavity has an important effect on the polymer brush conformation. A direct comparison between the SCF and MC methods reveals the SCF calculation to be a valuable alternative to MC simulations in the case of free and softly compressed brushes. In the case of strongly compressed systems we have proposed an extension of the Flory theory for polymer solutions, whose predictions are found to be in good agreement with the MC simulations and has the advantage of being computationally inexpensive. In the range of high compressions, we have found the monomer volume fraction v to follow a scale relationship with the cavity pressure P , $P \sim v^\alpha$. SCF calculations give $\alpha = 2.15 \pm 0.05$, close to *des Cloiseaux law* ($\alpha = 9/4$), whereas MC simulations lead to $\alpha = 2.73 \pm 0.04$. We conclude that the higher value of α obtained with MC comes from the monomer density correlations not included in the SCF formalism.

PACS numbers:

I. INTRODUCTION

The structure and dynamics of polymer chains terminally anchored or end-grafted to a surface is a very interesting problem from both, theoretical and experimental points of view, due to the inherent complexity of having chain molecules located in constrained geometrical environments. These polymer systems are relevant in many areas of polymer science and technology[1, 2], such as chromatography, surfactants, lubrication, adhesion, stabilization of colloidal systems, or even as potential drug carriers[3, 4, 5, 6]. Properties related to these systems are also of interest in the synthesis of nanoparticles[7]; spherical brushes formed by colloidal poly-(methyl methacrylate) spheres with a grafted layer of poly(12-hydroxy stearic acid) (PMMA-PHSA) have served as a model to emulate hard-spheres minimizing the effect of van der Waals forces [8]. More recently, the use of the light-scattering properties of coated spherical particles has been found to be a useful non-destructive way to probe and size systems ranging from blood cells to paper whiteners [9].

Former theoretical studies by de Gennes and Alexander[10, 11], Semenov [12], Milner-Witten-Cates[13, 14] and Zhulina-Priamitsyn-Borisov[15] focused on polymer chains grafted onto planar surfaces, and their predictions have been well supported by Monte Carlo[16, 17, 18, 19] and molecular dynamics[20] simulations.

The introduction of curved interfaces result in polymer brush structures whose properties differ significantly

from those expected from flat interfaces. Whereas the problem of concave surfaces, in which the surface curves towards the polymer chain, was solved by Semenov[21], for convex surfaces it has not been possible to find a potential form that provides a self-consistent solution leading to physical solutions. In this case, the increased volume available to the stretched polymer, as it moves away from the interface, is responsible of a rich physical behavior. For instance, colloidal silica spheres with grafted alkane chains undergo a sol-gel transition when dispersed in hexadecane solution[22].

On the other hand, experimental studies on the rheological properties of spherical brushes appear rather scarce, certainly due to the strong difficulties in the control of the grafting procedure[23]. Nonetheless, several studies using SANS [24, 25], ESR [26, 27] or NMR [28, 29] technics have dealt with the physical chain-properties of terminally attached homopolymers onto colloidal particles.

¿From the theoretical point of view, there have been several attempts to determine the interaction between spherical brushes. Daoud-Cotton[30] and Witten-Pincus[31] in the limiting case of star shaped polymers; Borukhov and Leibler[32] using the Derjaguin approximation valid for small curvature effects and short polymer chains. Several numerical studies have been devoted to the study the properties of single non-interacting brushes[33, 34, 35] and the interaction between two spherical brushes[36, 37].

Whereas the previous studies have analysed the properties of a single or two interacting spherical brushes, the understanding of the more complex and interesting problem of a system of colloidal spherical brushes in solution remains untouched. Particularly, in the limiting case of high densities, the colloidal brushes are subject to an isotropic pressure. In such case, the interaction of

*Email addresses: J. J. Cerda: jcerda@imedea.uib.es; T. Sintés: tomas@imedea.uib.es; R. Toral: raul@imedea.uib.es

a colloidal particle with the rest of the system can be modelled, in a first approximation, by a single spherical brush confined inside a spherical cavity. This model has the advantage of reducing the high computer cost. On the other hand, this model turns out to be relevant to the study of the properties of encapsulated dendrimers, liposomes, vesicles containing nanoparticles with grafted chains, and might be of relevance in the synthesis of polymer-grafted metal nanoclusters inside small material cavities or molecular cages.

The purpose of the present paper is to present the results of extensive MC and SCF simulations of a single colloidal brush confined inside a spherical cavity wall of variable radius. Polymer chains have an extent of the same order of the core size of the colloidal particle, such that curvature effects are important. We have measured the monomer density profile and the cavity pressure at different cavity radius. The results using MC and SCF methods have been compared at low and high compression regimes, discussing the advantages of each method.

The rest of the paper is organized as follows: in section II we describe the numerical procedures used to compute the monomer density profile and the cavity pressure; in section III we present a detailed analysis of the numerical calculations, this section also includes an extension of the Flory theory for a free polymer solution, as an alternative way to obtain the pressure inside the cavity; section IV concludes with a brief summary and a discussion of the results.

II. NUMERICAL MODELS

A. Monte Carlo method

In order to simulate the interaction between a spherical brush confined inside a spherical cavity wall, we have used a 3-dimensional off-lattice Monte Carlo method (MC). We have generated the brush by homogeneously distributing f polymer chains grafted onto an impenetrable spherical surface of radius r_c . The cavity wall is also impenetrable with a variable radius R . The polymer chain is represented by the pearl necklace model[38] containing N beads of diameter σ . The distance between two consecutive beads in the chain is set to 1.1σ . In all the simulations we have set $\sigma = 1$. The initial configuration of the self-avoiding polymer is randomly generated being the first monomer permanently anchored to the surface (it is never allowed to move). An schematic representation of the system is shown in Figure 1.

Monomers interact through a steric hard-core potential of the form:

$$U_{steric} = \sum_{i,j=1}^{N \times f} V(r_{ij}), \quad (1)$$

where V is a hard sphere potential:

$$V(r_{ij}) = \begin{cases} 0 & \text{for } |\mathbf{r}_i - \mathbf{r}_j| > \sigma, \\ \infty & \text{for } |\mathbf{r}_i - \mathbf{r}_j| < \sigma. \end{cases} \quad (2)$$

Different polymer configurations are generated by changing the position of a randomly selected monomer. If the monomer is located inside the chain (between the first monomer, permanently anchored, and the last one) its position changes by rotating an arbitrary angle between 0 and 2π around the axis connecting the previous and following monomers in the chain. Chain ends just perform random wiggling motions. The proposed motion is accepted if the excluded volume interaction is preserved (Eq. 2). A link-cell method [39] has been implemented in the algorithm to efficiently check all possible monomer overlaps.

Initially, the radius of the cavity wall is set to be larger than the usual extent of the brush to ensure that during the equilibration process no interaction between the brush and the cavity wall occurs. We define one Monte Carlo Step (MCS) as $N \times f$ trials to perform monomer moves. The spherical brush has been equilibrated typically during 5×10^5 MCS. After this initial equilibration time, magnitudes of interest are recorded every 10 MCS. In what follows, the expression for the force and interacting potential are given in units of $k_B T$.

The force that the system exerts to avoid compression is computed as the change in the free energy \mathcal{F} due to an infinitesimal change in the cavity radius R is given by:

$$F(R) \equiv \frac{\partial \ln Z(R)}{\partial R}, \quad (3)$$

where $Z(R) = \exp(-\mathcal{F}/k_B T)$ is the partition function of the system. Due to the hard-core structure of the potential, see Eq.(2), the partition function

$$Z(R) = \int \prod_{i=1}^{N \times f} d\mathbf{r}_i \exp\left(-\sum_{j=1}^{N \times f} V(\mathbf{r}_{ij})\right) \quad (4)$$

is equal to the volume $\Omega(R)$ of all possible polymer chains configurations compatible with the steric requirements.

Let $\Omega_C(R) \subset \Omega(R)$ be the subset of configurations compatible with a reduction of the radius cavity by an amount δR . Similarly, let $\Omega_E(R - \delta R) \subseteq \Omega(R - \delta R)$ be the set of polymer configurations of $\Omega(R - \delta R)$ in which it is possible to increase the radius of the cavity by an amount δR . The compression probability is just $P_C(R) = \Omega_C(R)/\Omega(R)$, and the probability that an expansion can be done is $P_E(R - \delta R) = \Omega_E(R - \delta R)/\Omega(R - \delta R)$. Since no steric requirement can prevent the expansion of the cavity, $P_E(R) = 1$ for all values of R . The subsets $\Omega_C(R)$ and $\Omega_E(R - \delta R)$ are in one to one correspondence, consequently

$$\frac{Z(R)}{Z(R - \delta R)} = \frac{\Omega(R)}{\Omega(R - \delta R)} = \frac{P_E(R - \delta R)}{P_C(R)} = \frac{1}{P_C(R)} \quad (5)$$

Because of the finite step δR used in computer simulations, we approximate

$$\frac{\partial \ln Z(R)}{\partial R} \approx \frac{1}{\delta R} \ln \frac{Z(R)}{Z(R - \delta R)} = \frac{-1}{\delta R} \ln P_C(R) \quad (6)$$

The compression probabilities are obtained by spanning directly this probability for a given cavity size R . Then, we force to compress the system to a new cavity size $R - \delta R$. The system is equilibrated again during 10^5 MCS before new measurements are taken.

The monomer radial density ϕ is defined as usual:

$$\phi(r) = \frac{\nu(r)}{4\pi r^2 dr}, \quad (7)$$

being $\nu(r)$ the number of monomers located within a distance between r and $r + dr$ from the centre of the sphere. The definition of $\phi(r)$ is such that the following normalization holds:

$$\int_0^\infty d^3r \phi(r) = Nf \quad (8)$$

In a similar way, we also define the chain-ends monomer density, $\epsilon(r)$, where $\nu(r)$ takes only into account the number of free chain ends.

B. Self Consistent Field method

In order to compute the probability density function (pdf) for polymer systems, it is customary to deal with a Schrödinger-like equation for the pdf for a single chain[40]. The use of this formalism is a valid approximation for spatial scales much larger than the polymer blob size. However, for encapsulated polymer brushes, and mainly at moderate and high compressions, the spatial scale of the cavity is comparable to the blob size. Thus, the use of the precedent formalism to compute the pdf becomes inadequate. Instead, we compute the pdf of a polymer chain using directly the recurrence law for the pdf from which the Schrödinger-like equation derives[40]. We must be aware that the use of the recurrence law still implies some approximations. It is assumed that on each monomer of the polymer chain acts a potential that only depends on the position of the monomer in the system, $U = U(\mathbf{r})$, therefore, bond correlations are not taken into account. It is also assumed that the potential is a function of the local monomer density, $U(\phi(\mathbf{r}))$, ignoring particle density correlations. Finally, the properties of the whole ensemble of chains are deduced from the pdf of a single chain.

Under the above assumptions, the spherical cavity is discretized in concentric shells of thickness dr and all monomers inside a shell are assumed to be equivalent. A polymer chain composed by N monomers is represented as a path of N segments of length σ . Each segment is labeled by an index τ associated to the spherical shell at which it belongs. The pdf associated to all possible paths

composed by n segments, being the first segment inside the shell \mathbf{h}' and the last one inside the shell \mathbf{h} , is defined as

$$G_n(\mathbf{h}', \mathbf{h}) \equiv \sum^A e^{-\sum_{i=1}^n U(\tau_i)} \quad (9)$$

in which \sum^A stands for a sum over all the hypothetical n -paths that join the shells \mathbf{h}' and \mathbf{h} . This function verifies $G_n(\mathbf{h}', \mathbf{h}) = G_n(\mathbf{h}, \mathbf{h}')$. Therefore, the pdf associated to a path of $n + 1$ segments may be written as

$$G_{n+1}(\mathbf{h}', \mathbf{h}) = \sum^A \left(e^{-\sum_{i=1}^n U(\tau_i)} e^{-U(\tau_{n+1})} \right) \quad (10)$$

Assuming $U(\tau_{n+1})$ to be independent of rest of the segments in the chain and of the starting point of the sequence, the precedent equation reads:

$$G_{n+1}(\mathbf{h}', \mathbf{h}) = \left(\sum_{\mathbf{h}''}^D G_n(\mathbf{h}', \mathbf{h}'') \right) e^{-U(\mathbf{h})} \quad (11)$$

where \sum^D implies a sum over all the \mathbf{h}'' shells from which we can get into shell \mathbf{h} using a single segment, therefore, shells \mathbf{h}'' and \mathbf{h} are at a relative distance less or equal to σ . The above equation stands for the recurrence law needed to calculate the chain pdf once the potential $U(\mathbf{h})$ is given.

We have set the interaction potential $U(i)$ to be proportional to the monomer concentration in shell i , $\phi(i)$:

$$U(i) = \omega \phi(i) \quad (12)$$

where w is the excluded volume parameter defined as[41]:

$$\omega = 4\pi \int_0^\infty (1 - e^{-V(r)}) r^2 dr \quad (13)$$

where $V(r)$ is the interaction potential introduced in Equation (2), that for a value of $\sigma = 1$, as in the MC method, we obtain $\omega = 4\pi/3 \approx 4.2$

The monomer concentration $\phi(i)$ and the free-end-chain concentration $\epsilon(i)$ are defined as:

$$\phi(i) = \frac{f}{4\pi r_i^2 dr} \frac{e^{U(i)} \sum_{n=0}^{n=N} \sum_{j=i_{r_c}}^{i_{R}} G_n(i_{r_c}, i) G_{N-n}(i, j)}{\sum_{j=i_{r_c}}^{i_{R}} G_N(i_{r_c}, j)} \quad (14)$$

$$\epsilon(i) = \frac{f}{4\pi r_i^2 dr} \frac{G_N(i_{r_c}, i)}{\sum_{j=i_{r_c}}^{i_{R}} G_N(i_{r_c}, j)} \quad (15)$$

where f is the number of chains and i_{r_c} and i_R are the shell indexes with radius equal to the brush core surface and the cavity wall respectively. The factor $e^{U(i)}$ in the monomer concentration is introduced to avoid double counting of the interaction term $e^{-U(i)}$ at shell i that comes from splitting the pdf into two terms, one that ends at shell i and the other starting at the same shell.

The change in the free energy when we reduce the cavity size, $\Delta\mathcal{F}(i_R)$, is given by

$$\Delta\mathcal{F}(i_R) = \ln\left(\frac{\Omega(i_R)}{\Omega(\infty)}\right) \quad (16)$$

being

$$\Omega(i) = f \sum_{j=i_{r_c}}^i G_N(i_{r_c}, j). \quad (17)$$

We have set the reference state as a system with a cavity wall at a distance far enough so that no chain can reach this wall. Therefore, the force to compress the brush, given a cavity size R , is:

$$F(R) = -\frac{\partial(\Delta\mathcal{F}(R))}{\partial R} \quad (18)$$

Given R , N and f , an iterative process is used to obtain the pdf and the density profiles. We have iterated the process until self-consistency is reached. We set the condition for self-consistency such that the sum of the square differences in the density profiles coming from two consecutive iterative steps is less than 10^{-8} .

The SCF method has the great advantage of being three to four orders of magnitude less expensive in computer time than the MC method. In the next section we will show that SCF and MC calculations give similar results for the density profiles $\phi(r)$ and $\epsilon(r)$ in the case of free polymer brushes. However, SCF predictions for the cavity pressure worsen for highly compressed systems.

III. RESULTS AND DISCUSSION

A. Density profiles

We have performed extensive numerical calculations for free and encapsulated spherical polymer brushes in order to compute the monomer density profiles and the compression forces for different sets of parameters (R, N, f) . The core radius of the colloidal particle where polymers are grafted is taken to be $r_c = 5\sigma$ and is kept constant through all the simulations. The diameter of the monomers is set to $\sigma = 1$. We have taken polymer chain lengths in the range of $N = 30$ to $N = 70$, and we have varied the number of grafted chains from $f = 5$ to $f = 75$. The range of parameters (N, f) has been chosen in order to obtain chain extents roughly of the same order than the diameter of the core where curvature effects are important. For the SCF method we have used a shell thickness $dr = 0.1\sigma$.

We have first studied the monomer density profiles $\phi(r)$ for an unconstrained spherical brush using our MC simulations and the SCF formalism. In Figure 2 we present the results for two different values of the chain length N and number of grafted chains f that correspond to representative values for soft and densely packed brushes. We can observe a good agreement between the MC and SCF

calculations. The density oscillations observed at small r , close to the core of the colloidal particle, are originated due to wall-effects of the impenetrable core. For a free spherical polymer brush Cariagno and Szeleifer[42] computed the monomer density profile derived from a single-chain mean field theory. A comparison between the Cariagno and Szeleifer data (CS) and our results is also included in Figure 2. The better agreement of the CS predictions with our MC simulations, in contrast to the SCF calculations, can be understood in the sense that the Cariagno and Szeleifer formalism requires a representative sample of chain configurations as an input data to solve the equations that we have generated using our MC method.

In Figure 3 we compare the monomer and chain-end density profiles for unconstrained polymer brushes obtained from our MC and SCF calculations. Figure 3(a) stands for $N=30$ and $f=25$, whereas Figure 3(b) and Figure 3(c) show the results for $(N=30, f=75)$ and $(N=50, f=75)$ respectively. In all cases the profiles are roughly similar. In particular, both methods agree very well in the case of the chain-end density profile $\epsilon(r)$ for short chains in a densely packed brush (see inset of Figure 3(b)). This is mainly due to the fact that the chains are forced to be mostly fully stretched out and density correlations, not present in the SCF formalism, are not relevant. On the other hand, the results for the monomer density profiles $\phi(r)$ show systematic differences, although small, between the MC and SCF calculations. Close to the core of the colloidal brush, SCF results display density profiles slightly smaller than those obtained via MC simulations. And vice versa, in an intermediate region, the SCF method gives densities slightly larger than in the MC simulations. The same systematic behaviour was found by Cosgrove et al.[44], when comparing MC and SCF density profiles for flat brushes. Cosgrove attributed these differences to the fact that MC simulations account explicitly for the excluded volume effect, whereas SCF accounts only approximately for this effect.

B. Cavity pressure and force profiles

We have measured the force profile exerted by an encapsulated spherical polymer brush onto the external cavity wall through the evaluation of the changes in the free energy due to an infinitesimal change in the radius of the cavity. Within the MC simulations, the force can be calculated by directly measuring the compression probabilities (Equation 6); whereas in the SCF approach, once we have reached self-consistency, we use the pdf in Equations 16 to 18.

Alternatively, we propose another way to compute the force profile and the cavity pressure that is derived from the Flory theory for polymer solutions[43]. This method has the advantage of being computationally inexpensive, and their predictions will be compared with the MC and

SCF calculations.

An extension of the Flory theory for polymer solutions

In the Flory theory the osmotic pressure in a polymer solution can be written as:

$$\Pi(R) = \frac{-1}{\mathcal{V}} \left(\ln(1-v) + \left(1 - \frac{1}{N}\right)v + \chi v^2 \right) \quad (19)$$

where \mathcal{V} is the molar volume of the solvent, v is the volume fraction of solute, N is the degree of polymerization or chain length, and χ is the Flory parameter. We set $\chi = 0$ which is the condition of a dry-brush. Under this assumption, the contributions to the free energy come only from the entropy associated to all possible configurations of the system. We suppose that the volume of the solvent and the volume fraction of the solute are given respectively by:

$$\mathcal{V} \sim (\tau - aNf) \quad (20)$$

$$v = \frac{aNf}{\tau} \quad (21)$$

a is the volume of a single monomer. τ is the total available cavity volume between the inner wall, represented by the core of the colloidal particle where chains are grafted and the cavity wall, thus:

$$\tau(R) = \frac{4\pi}{3}(R^3 - r_c^3) \quad (22)$$

At variance with the original Flory treatment, the molar volume of the solvent \mathcal{V} refers to the remaining space in the system once we have subtracted the volume occupied by the monomers, thus, it is no longer a constant value.

The force to compress the cavity will be proportional to the area of the cavity wall and to the change in the osmotic pressure, thus:

$$F(R) \sim 4\pi R^2 \Delta\Pi(R) \quad (23)$$

In Figures 4 to 6 we present in log-log plots the force profile $F(R)$ vs. the cavity size R computed for different values of the polymer chain length N and number of grafted chains f . In each figure we include the results coming from the MC simulations (circles), the predictions of the SCF theory (dashed lines) and results derived from the application of the extended Flory theory (crosses). Figure 4 concentrates on the results derived for short polymer chains ($N = 30$); Figure 5 for intermediate chain lengths ($N = 50$); and Figure 6 for long polymers ($N = 70$). In all the cases studied we have used the same fitting constant to adjust the predictions of the extended Flory theory (see Eq. 23), and we have taken, as a reference state, a cavity size R^* at which $\ln(F(R^*)) \rightarrow -\infty$ in the MC simulations.

A direct comparison between SCF and MC force profiles shows a rather good agreement for weakly compressed systems. However, systematic differences are observed for intermediate and high compression values. In the intermediate region we found the SCF forces to be larger than the ones derived from the MC simulations, whereas for high compressions it is the MC force the one that becomes larger than the SCF outcome.

The mismatches observed between the SCF and MC results are due to a twofold effect. For small cavity sizes or highly compressed systems, the assumption in the SCF model of a linear dependence of the mean field potential with the monomer density (see Eq. 12) breaks down. In fact, under this assumption, the SCF formalism allows a cavity size smaller than the volume occupied by the polymers without requiring an infinite force. On the other hand, for intermediate compression values, the larger forces obtained with the SCF formalism are originated in an overestimation of the monomer interactions. The SCF method does not include the effect of monomer correlations, thus it allows higher average densities in the system than the ones found in the MC simulations. As a consequence, stronger repulsions between the polymers take place and a higher force is required to compress the brush.

The predictions of the extended Flory theory are found, remarkably, despite its simplicity, to be in a very good agreement with the results of the MC simulations in the intermediate and high compression regimes. However, the force is overestimated for weakly compressed systems. This result is easily explained since the Flory theory was formerly developed for free polymer chains. As the cavity size grows, the difference between a system of grafted chains and a polymer solution becomes evident and, as it is expected, the interaction of the grafted chains with the outer surface is much weaker than the one coming from a polymer solution.

It is worth to notice that the MC data can be fitted remarkably well with the extended Flory theory for intermediate and high compression values, and with the SCF formalism for weakly compressed systems.

We have analysed the relationship between the monomer volume fraction v (see Eq. 21) and the pressure exerted on the cavity wall P defined as the force to compress the system divided by the area of the cavity. The results for the MC and SCF calculations are shown in log-log plots in Figure 7 and Figure 8 respectively. In both cases, we find a complex behavior of the monomer volume fraction with the cavity pressure for weakly compressed systems that depends on the different values of the polymer chain length N and number of grafted chains f . But, for increasing values of the cavity pressure v and P follow a power-law of the form $P \sim v^\alpha$ independent of N and f . The best fit to the numerical data gives a slope of $\alpha = 2.73 \pm 0.04$ for the MC simulations and $\alpha = 2.15 \pm 0.05$ for the SCF results. The exponent obtained for the SCF data is very close to the des Cloiseaux power law ($\alpha = 9/4$) found in semi-dilute polymer solu-

tions [40]. For large monomer concentrations the polymer theory predicts that all thermodynamic properties must reach values that are independent of the degree of polymerization, as we have observed in both MC and SCF methods. We must be aware that des Cloiseaux law is deduced from scaling arguments and neglects non-linear dependences on the concentration. This fact might explain the agreement between SCF and des Cloiseaux law, whereas MC results follows a power law which exponent is larger due to monomer density correlation effects.

Differences between force profiles derived from SCF formalisms, and those obtained from other methods that account for chain interdigitation and correlations between the nearest-neighboring bonds are also referenced in several works. For instance, Ruckenstein-Li[45] (to be referred as RL) compared the experimental force profile of two interacting crossed cylinders bearing grafted polymer chains, with the numerical data obtained with a generator matrix formalism and from SCF methods. RL found the matrix formalism to provide a better agreement with the experimental data than the SCF results. In most cases, the force profiles derived by RL with the matrix formalism and the SCF method are rather similar to the ones we found comparing the MC simulations and the SCF calculation. This reinforces our presumption that interdigitation and monomer correlations are responsible of the observed differences between the MC and SCF data. Additionally, the fact that mean field calculations overcounts the segment-segment interactions in the evaluation of the free energy, as mentioned above, has already been noticed by Lin and Gast [46].

IV. SUMMARY AND CONCLUDING REMARKS

In this paper we have studied the behavior of an encapsulated spherical brush inside a spherical cavity. This system is a first approximation to model the interactions in a solution of colloidal particles bearing grafted polymer chains onto their surface. This model is particularly relevant for moderate and high density values where the colloidal brushes are subject to an isotropic pressure, and might be of relevance to the behavior of encapsulated dendrimers, liposomes or vesicles containing polymer brushes as well.

We have measured the monomer density profile and the cavity forces through extensive 3-dimensional off-lattice Monte-Carlo simulations and using a Self-Consistent Field formalism. In the latter case, we have used directly the probability density function recurrence law for the propagator $G_N(r, r')$, avoiding the length scale approximation involved in self-consistent field methods that

uses Schrödinger-like equations. Alternatively, we have proposed a theoretical description based on an extension of the Flory theory for polymer solutions to compute the pressure inside the cavity.

A comparison of the predicted forces exerted by the polymer brush onto the cavity surface among the different methods reveals the following: *i*) For weakly compressed systems, MC and SCF data show a rather good agreement. However, the force is overestimated in the extended Flory theory. This difference arises since the Flory theory was developed for free polymer chains and not for polymer brushes, thus, its prediction is not physically relevant when the cavity wall is located at a distance larger than the typical brush extension. *ii*) For intermediate and highly compressed systems the MC data agrees reasonably well with the results derived from the Flory theory. In the intermediate regime, it is the SCF formalism that overestimate the force. This behavior can be easily explained since the SCF method does not account for monomer correlations, allowing higher monomer densities and thus, higher forces are required to compress the brush. On the other hand, for highly compressed systems, the linear dependence of the mean field potential with the monomer density turns out to be inadequate (the repulsion between monomers allows a volume reduction of the system beyond the own excluded volume of the monomers at a finite energy cost) leading to lower forces than the ones derived from MC simulations.

We have found a power law relationship between the monomer volume fraction and the cavity pressure, $P \sim v^\alpha$. SCF data gives a slope of $\alpha = 2.15$, very close to the des Cloiseaux law derived for semi-dilute polymer solutions. On the other hand, the MC simulations provide a larger exponent $\alpha = 2.73$ that is originated in the monomer correlations not present in the previous models.

The study of a spherical brush constrained by an isotropic steric wall is directly related to the problem of a dense solution of colloidal particles with grafted chains onto their surface where chain interdigitation among brushes is not favoured. We expect these results to stimulate further theoretical and experimental studies towards the understanding of the behaviour of colloidal particle systems in solution. In this sense, the computed force can be directly related to the measure of disjoint pressures by using the expressions derived by Evans and Napper[47].

Acknowledgments

Financial support from the Spanish MCyT grants nos. BFM2000-1108 and BFM2001-0341-C02-01 are acknowledged.

[1] Napper, D. H. *Polymeric Stabilization of colloidal dispersion*; Academic, London, 1983.

[2] Russel, W. B; Saville, D.A. and Schowalter, W.R. *Col-*

- loidal Dispersions*; Cambridge University Press, Cambridge, 1989.
- [3] Hsu, W. P.; Yu R. and Matijevic, E., *J. of Colloid Interface Sci.* **1993**, 156, 36.
- [4] Meyer, R. A., *Appl. Opt.*, **1979**, 18, 585.
- [5] van Zanten, J. H. and Monbouquette, H. G., *J. Colloid Interface Sci.* **1991**, 146, 330.
- [6] Kuhl, T. L. ; Leckband, D. E.; Lasic D. D.; and Israelachvili, J. N., *Biophys. J.* **1994**, 66, 1479.
- [7] Mangeney, C. ; Ferrage, F.; Aujard I. et al, *J. Am. Chem. Soc.*, **2002**, 124, 5811.
- [8] Phan, S. ; Russel, W. B.; Cheng, Z.; Zhu, J.; Chaikin, P. M.; Dunsmuir J. H.; and Ottewill, R.H., *Phys. Rev. E* **1996**, 54, 6633.
- [9] Quirantes, A.; and Delgado, A. V., *J.Phys.D: Appl. Phys.* **1997**, 30, 2123.
- [10] de Gennes, P. G., *J. Phys.(Paris)*, **1976**, 37, 1443; *Macromolecules*, **1980**, 13, 1069; *C. R. Acad. Sci. (Paris)*, **1985**, 300, 839.
- [11] Alexander, S., *J. Phys.(Paris)*, **1977**, 38, 983.
- [12] Semenov, A. N., *Sov. Phys. JETP*, **1985**, 61, 733.
- [13] Milner, S. T.; Witten T. A.; and Cates M. E., *Macromolecules* **1998**, 21, 2610; *Europhys. Lett.*, **1988**, 5, 413; *Macromolecules* **1989**, 22, 853.
- [14] Milner, S. T.; and Witten, T. A., *J. Phys.(Paris)*, **1998**, 49, 1951.
- [15] Zhulina, E. B.; Borisov O. V.; and Priamitsyn, V. A., *J. Colloid Interface Sci.*, **1990**, 137, 495.
- [16] Chakrabarti, A.; and Toral R., *Macromolecules*, **1990**, 23, 2016.
- [17] Lai, P.Y.; and Binder, K., *J. Chem. Phys.*, **1991**, 95, 9288.
- [18] Toral, R.; Chakrabarti, A.; and Dickman, R., *Phys. Rev. E*, **1994**, 50, 343.
- [19] Chakrabarti, A.; Nelson P.; and Toral, R., *Phys. Rev. A*, **1992**, 46, 4930; *J. Chem. Phys.* **1994**, 100, 748.
- [20] Murat, M.; and Grest, G.S., *Macromolecules*, **1989**, 22, 4054; *Phys. Rev. Lett.* **1989**, 63, 1074.
- [21] Semenov, A. N.; *Sov. Phys. JETP*, **61**, 733, (1985) (*Zh. Eksp. Teor. Fiz.*, **1985**, 88, 1242).
- [22] Grant, M. C.; Russel, W. B., *Phys. Rev. E*, **1993**, 47, 2606.
- [23] Nommensen, M. H.; Duits, G.; van den Ende, D.; and Mellema, J., *Phys. Rev. E*, **1999**, 59, 3147.
- [24] Cosgrove, T.; Crowley, T.L; Vincent, B.; Barnett K.G.; and Tadros, Th. F., *Faraday Discussions*, **1982**, 16, 101.
- [25] Beaufils, J.P.; Hennion, M.C.; and Rosset, R., *J. de Physique*, **1983**, 44, 497.
- [26] Hommel, H.; Legrand, A.P; Balard, H.; and Papirer, E., *Polymer*, **1983**, 24, 959.
- [27] Hommel, H.; Legrand, A.P., J. le Courtier and J. Desbarres, *Eur. Polym. J.*, **1979**, 15, 993.
- [28] Gilpin, D. K.; and Geindoga, E., *J. Chromatogr. Sci.*, **1983**, 21, 352.
- [29] Cosgrove, T.; Vincent, B.; Stuart, M. C.; Barnett, K.G.; and Sissons, D.S., *Macromolecules*, **1981**, 14, 1018.
- [30] Daoud, M.; and Cotton, J. P., *J. Physique*, **1982**, 43, 531.
- [31] Witten, T. A.; and Pincus, P. A., *Macromolecules*, **1986**, 19, 2509.
- [32] Borukhov, I.; and Leibler, L., *Phys. Rev. E*, **2000**, 62, R41.
- [33] Dan, N.; and Tirell, M., *Macromolecules*, **1992**, 25, 2890.
- [34] Toral, R.; and Chakrabarti, A., *Phys. Rev. E*, **1993**, 47, 4240.
- [35] Grest, G.S.; and Murat, M., *Macromolecules* **1993**, 26, 3108.
- [36] Wijmans, C.M.; Leermakers, F.A.M.; and Fleer, G.J., *Langmuir* **1994**, 10, 4514.
- [37] Cerdà, J. J.; Sintes, T.; and Toral, R., *Macromolecules* **2003**, 36, 1407.
- [38] Baugärtner, A., in *Applications of the Monte Carlo Method in Statistical Physics*, 2nd ed. Edited by K. Binder. Topics in Current Physics 36. Springer-Verlag, Berlin, 1987.
- [39] Allen, M.; and Tildesley, D., *Computer Simulation of Liquids*; Clarendon, Oxford, 1987.
- [40] de Gennes, P. G., *Scaling concepts in polymer physics*; Cornell University, Ithaca NY, 1979.
- [41] Edwards, S.F., *Proc. Phys. Soc.*, **1965**, 85, 613.
- [42] Carignano, M.A.; and Szleifer, I., *J. Chem. Phys.*, **1995**, 102, 8662.
- [43] Flory, P. J. *Principles of Polymer Chemistry*; Cornell University Press, 1953.
- [44] Cosgrove, T.; Heath, T.; van Lent, B.; Leermakers, F.A.M.; and Scheutjens, J. M. H. M., *Macromolecules*, **1987**, 20, 1692.
- [45] Ruckenstein, E.; and Li, B., *J. Chem. Phys.* **1997**, 107, 3.
- [46] Lin, E.K.; and Gast, A.P., *Macromolecules*, **1996**, 29, 390.
- [47] Evans, R.; and Napper, D. H., *J. Colloid Interface Sci.* **1978**, 63, 43.

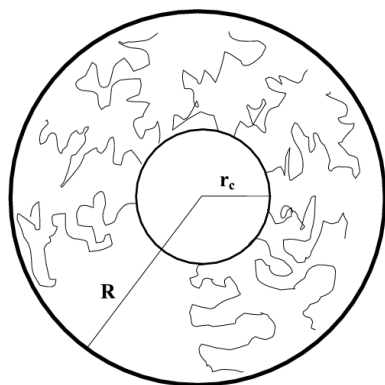


FIG. 1: Schematic representation of a spherical brush with an impenetrable core of radius r_c inside a spherical cavity of radius R .

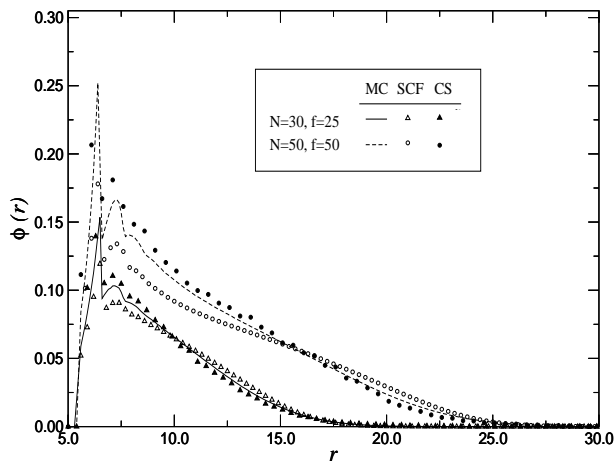


FIG. 2: Comparison between the monomer density profile $\phi(r)$ for free or uncompressed spherical polymer brushes obtained from our MC simulations (lines) and SCF calculations (symbols) for different values of the chain length N and number of grafted chains f . The results are compared to the predictions of Cariagno and Szeifer[42] (CS, filled symbols)

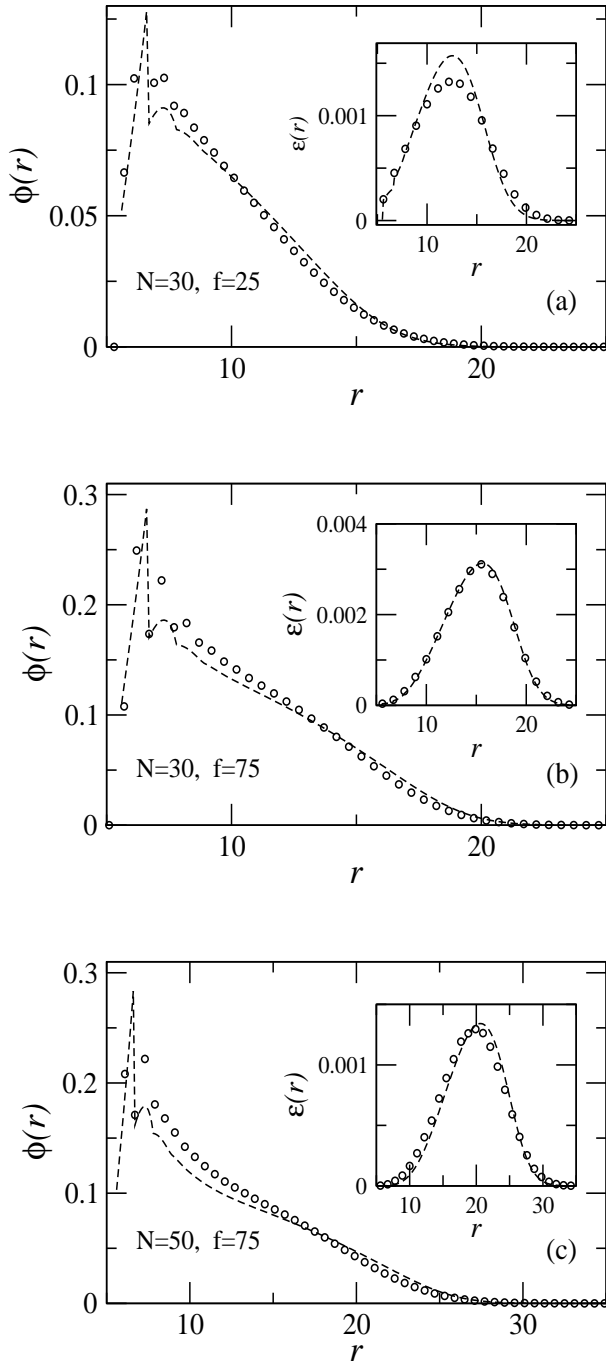


FIG. 3: Comparison between the monomer density profiles $\phi(r)$ for uncompressed spherical brushes obtained with MC (o) and SCF (dashed lines) calculations. Inset: chain-end density profiles. From top to bottom: (a) $N = 30, f = 25$; (b) $N = 30, f = 75$; (c) $N = 50, f = 75$.

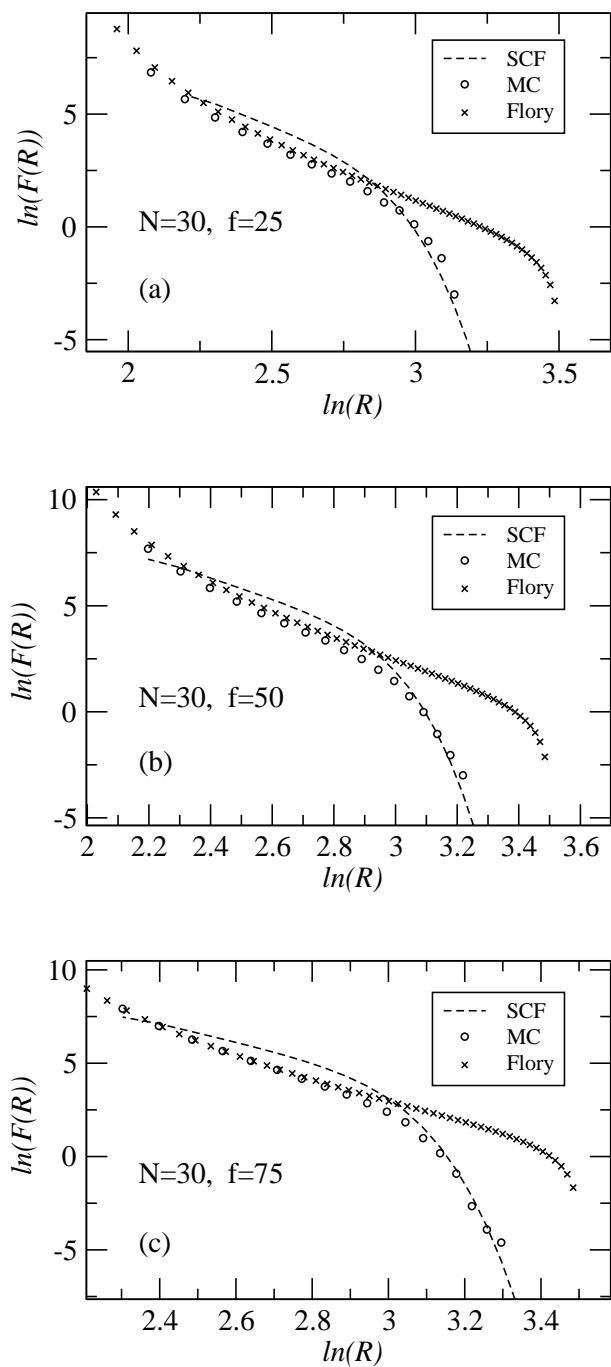


FIG. 4: Log-log plot of the force profile of an encapsulated spherical polymer brush vs. the cavity size R , for polymer chains of length $N = 30$. MC results are represented by filled circles; SCF data by dashed lines; and the predictions coming from the Flory theory by crosses. Different figures stand for different number of grafted chains f . From top to bottom: (a) $f = 25$; (b) $f = 50$; (c) $f = 75$.

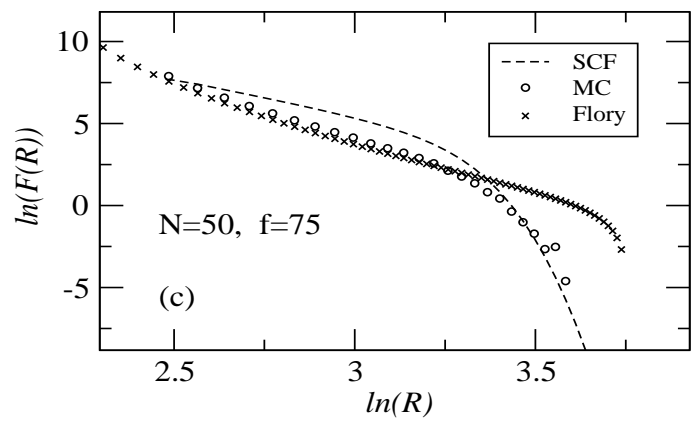
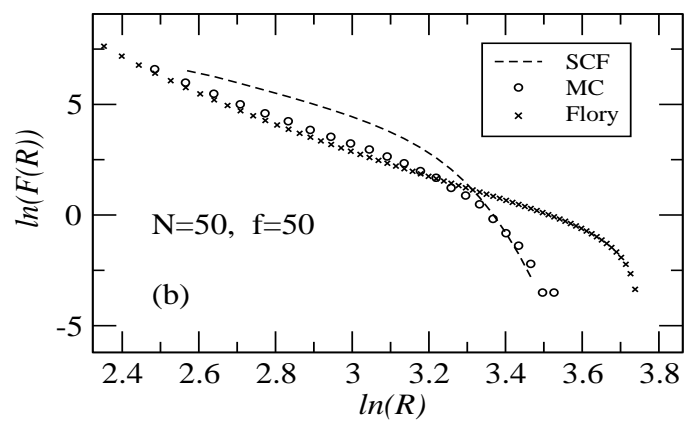
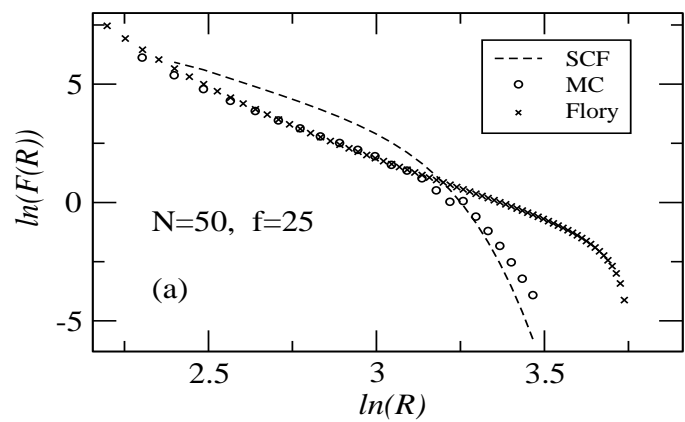


FIG. 5: Same as Figure 4 for polymer chains of length $N = 50$. From top to bottom: (a) $f = 25$; (b) $f = 50$; (c) $f = 75$.

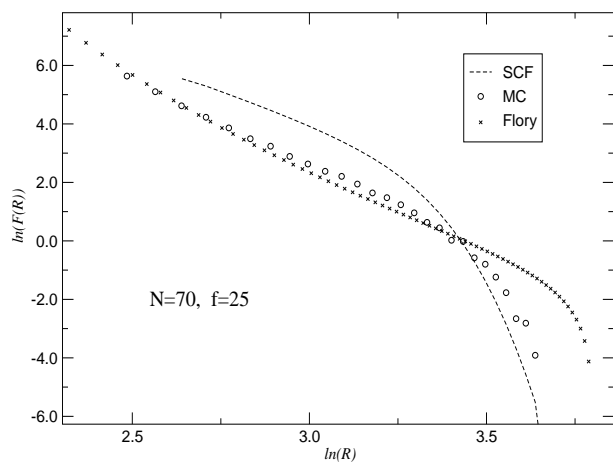


FIG. 6: Same as Figure 4 for the single case of long polymer brushes with $N = 70$ and $f = 25$.

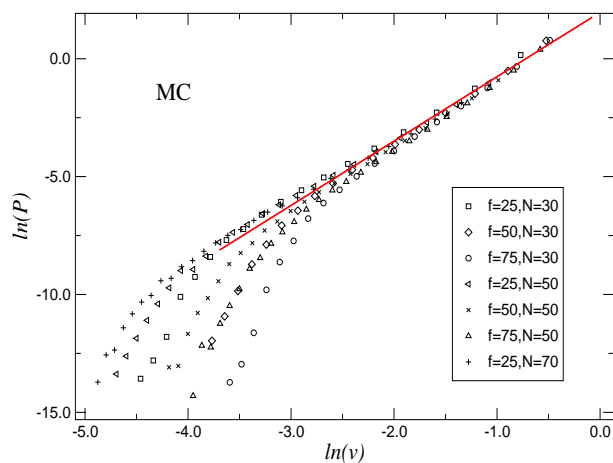


FIG. 7: Log-log plot of the system pressure P vs. the monomer volume fraction v obtained from MC simulations for different values of the chain length N and number of grafted chains f . A solid line of slope 2.73 is included to guide the eye.

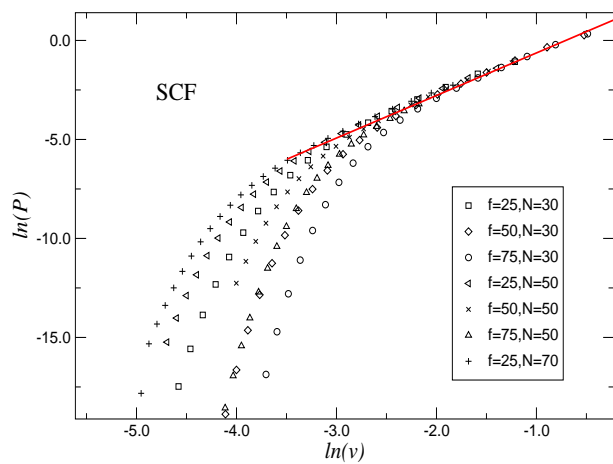


FIG. 8: Log-log plot of the system pressure vs. the monomer volume fraction v derived from the SCF formalism. A solid line of slope 2.15 is included to guide the eye.